# LIF MEASUREMENTS IN THE WAKE OF A BLUNT BODY IN HEG

**M. Rosenhauer, M. Wollenhaupt, M. Scheer and W.H. Beck**

*Institute for Fluid Mechanics German Aerospace Research Establishment DLR*
*Bunsenstr. 10, 37073 Göttingen, Germany*

## ABSTRACT

Laser induces fluorescence studies on NO were carried out in the wake region of a capsule placed in HEG flows. Temperature profiles along a line were determined at 2 positions downstream of the model. Contamination effects in HEG prevented an absolute temperature evaluation; thus results are presented as relative temperature changes which agree quantitatively with the expected flow features in the wake region.

**Keywords:** laser induced fluorescence, NO, high enthalpy, wind tunnel

## 1. INTRODUCTION

A space capsule entering a planetary atmosphere is subject to conditions on its windward face that are comparable to (or perhaps more severe than) those pertaining to a space glider reentering the Earth's atmosphere. For this reason, sensitive instrumentation is placed on the leeward side of the capsule. An examination of this (wake) region on the leeward side of the capsule is the subject of an AGARD study being carried out in cooperation with NASA in the High Enthalpy Shock Tunnel Göttingen (HEG) (see paper presented at this meeting [1]).

In this paper, the first attempts at carrying out laser induced fluorescence (LIF) studies of NO in the capsule wake region in HEG (≈50 MPa burst pressure, enthalpy ≈11 MJ/kg) are presented. The fluorescence signals from the 2 lasers were spectrally resolved to ensure that there was no extraneous emission due to contamination; although this meant the loss of 2d resolution, images along a line (1d) could be obtained. Evaluation of the images yielded relative temperatures (NO $T_{rot}$) at 2 positions downstream of the model. Absolute temperatures are presently obscured by contamination in the flow and possible saturation effects.

## 2. SPECTROSCOPY

Spectroscopic transitions used for LIF in HEG need to satisfy the following criteria :

1. Single line or line pair of different branches from the same ground state;
2. $\Delta E \geq kT$,
   where $\Delta E$ denotes the energy difference between the two lower states;
3. excitation must be within the tuning range of the ArF excimer laser;
4. no overlap by $O_2$ absorption;
5. line intensity must be detectable with the imaging system;
6. no interference with HEG emission (Figure 1).

Some newly identified lines which meet these criteria are indicated by number in Figure 6. Lines used in HEG in this study are marked by circles. The $R_{21}(17.5)$ line, however, does not meet criterion 1 because it is overlapped with a $P_{11}(35.5)$ line. This has to be taken into consideration for quantitative evaluation. For future measurements in HEG other line pairs have to be investigated as well.

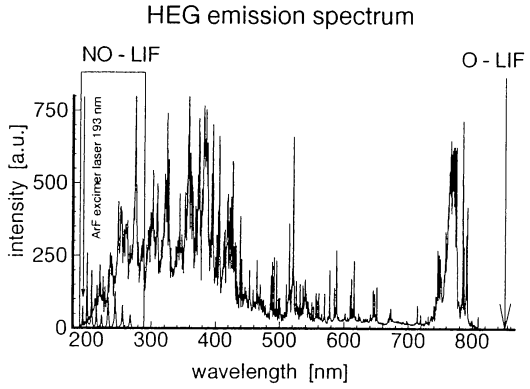


*Figure 1. HEG emission spectrum.*

A further problem in HEG is emission by contamination, spectra taken in the stagnation region of a cylinder flow in HEG (see Figure 1.) show profuse radiation down to 220 nm. In order to quantify this in the blunt body wake, all LIF images were recorded spectrally resolved.

*Proc. of the Second European Symposium on Aerothermodynamics for Space Vehicles, held in ESTEC, Noordwijk, The Netherlands, 21 – 25 November 1994 (ESA SP-367, February 1995)*

## 3. EXPERIMENTAL SETUP

The LIF apparatus is shown in Figure 7. and described elsewhere [2] in greater detail. The beams of two ArF excimer lasers, tuned to different transitions of NO, counterpropagate through the test section of the HEG and overlap in the wake of the model (Figure 2.). To increase laserpower in the probe region, the beams are focused with spherical lenses. A small percentage of the laser light is deflected to beam profile cameras to monitor laserpower during the shot.

The induced fluorescence of each laser is captured separately by its corresponding imaging system. These systems consist of an intensified gated CCD-camera plus UV-Nikkor lens and spectrograph which are used as an optical multichannel analyser (OMA) for spectrally resolved 1D imaging. The OMA slit is aligned parallel to the focused laser beam. In order to tune the lasers prior to the wind tunnel run and measure quantitatively the detuning (i.e. wavelength drift), a portion of the laser beams is deflected into a heated calibration cell containing NO.

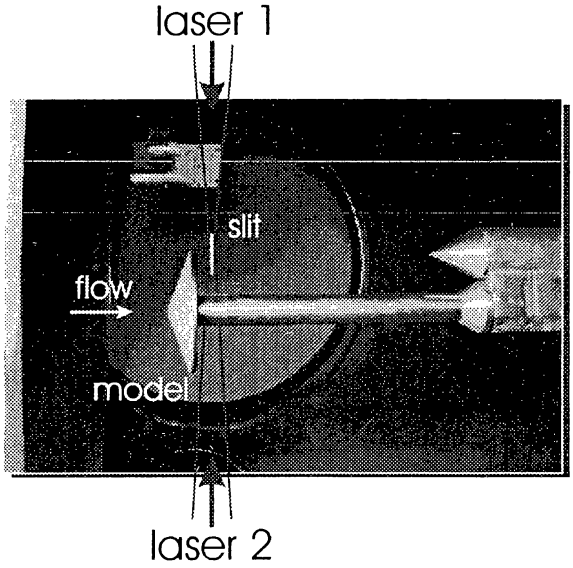


*Figure 2. Laser beam and OMA slit configuration for the blunt body model in HEG*

## 4. RESULTS AND DISCUSSION

LIF measurements were carried out for HEG shots #126-129 with the following conditions (Table 1).

| shot | $p_0$ [MPa] | $h_0$ [MJ/kg] | OMA slit pos. |
|---|---|---|---|
| 126 | 49.4 | 10.73 | 1 |
| 127 | 48.2 | 10.97 | 1 |
| 128 | 52.6 | 11.27 | 2 |
| 129 | 53.1 | 10.90 | 2 |

*Table 1. HEG test conditions*

Rotational temperatures were obtained by tuning the lasers to the $\varepsilon(0,1)$ $R_{21}(17.5)$ and $R_{22}(27.5)$ transitions, respectively. The OMA slit was oriented as shown in Figure 3.

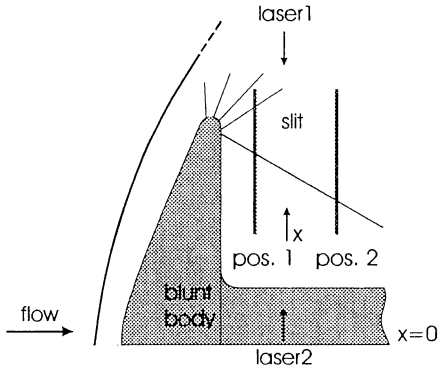


*Figure 3. Model with OMA slit positions*

For calibration of the system, the heated cell was installed inside the HEG test section and calibration of the used transitions at the known temperature $T_C$ was carried out.

Due to the focusing of the laser beams the transitions were partially saturated during calibration in the hot cell. The degree of saturation during shots in the HEG is not exactly known due to particle contamination of the flow. For this reason absolute temperatures still contain some uncertainty. This is expressed by the normalisation factor $T_{\text{linear LIF}}$ which is given here for the limit of linear LIF as ≈1800K.

Figure 4 shows camera images obtained from shot #129. Image 1 and 2 show the fluorescence arising from the excitation of the $\varepsilon(0,1)$ $R_{21}(17.5)$ and $\varepsilon(0,1)$ $R_{22}(27.5)$ transitions; fluorescence wavelength and distance x (see Fig. 6) along the OMA slit are plotted horizontally and vertically, respectively. The images clearly show NO $D(0)\rightarrow X(v'')$ fluorescence and $A(0)\rightarrow X(v'')$ cascade fluorescence. Emission of hot gas is negligible in the range of 190-270 nm. Image 3 displays the fluorescence of NO in the calibration cell during the shot which is used for the detuning correction. Images 4 and 5 compare the laser beam profiles before and after passing through the test section. It is obvious that strong absorption occurs due to contamination of the gas flow in the present time window.

LIF image data contain several systematic and random errors. Most of those cancel out after division of the two images and division with the calibration images (2). Some errors, however, have to be corrected in each image separately. In summary, the sequence employed for correcting systematic error in the recorded image is as follows. First, a combined image of the dark current and background signals is subtracted from the recorded image. This image is taken immediately after the shot.

Second, the laser power at the shot is included through a multiplicative factor (images 4, 5). Third, the detuning of the lasers between our last tuning with the NO fluorescence in the calibration cell and the shot is corrected by another multiplicative factor.

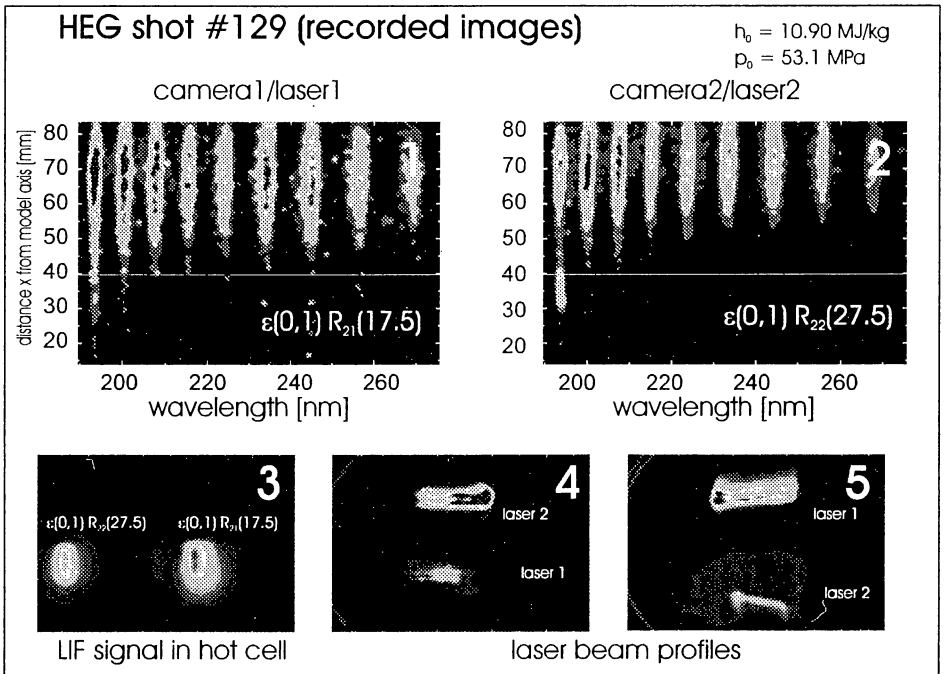


*Figure. 4 camera images of shot 129*

After these corrections the signal of one camera is given as:

$$I^i(T) = [NO] \cdot \frac{e^{-E^i/kT}}{Q(T)} \cdot q_F(A^i, Q^i) \cdot c(x,y) \quad (1)$$

with $E^i$ the transition energy of $[NO]_i$, the quantum yield $q_F$ with Einstein-coefficient $A^i$, the quenching rate $Q^i$, the transfer function $c(x,y)$ and the partition function $Q(T)$.

Given the ratio:

$$R = \left\{ \frac{I^1(T)/I^2(T)}{I^1(T_C)/I^2(T_C)} \right\} \quad (2)$$

with $T_C$ the calibration temperature, the temperature $T$ may be calculated from

$$T = \left\{ \frac{\ln(R)}{\Delta T} + \frac{1}{T_C} \right\}^{-1} \quad (3)$$

The advantage of the 2 level system is that we have to rely only on measured quantities.

In Figure 5 relative temperatures in the wake of the model along the OMA slit are shown. The spatial resolution is not good and especially for short distances from the model axis, the signal to noise ratio is poor. Nevertheless, it is still possible to discern some features in the wake: the temperature changes were rapidly at position 1, as expected, and both positions 1 and 2 have a region between x=50 and 70 mm where the temperatures are similar.

## 5. SUMMARY AND CONCLUSIONS

The spectrally resolved measurements demonstrate that the spectral emission of the hot gas in the wake is weak relative to the fluorescence signal, thus spectral filters will be used for in high resolution 2D measurements scheduled for March 1995 with the same model. Absolute temperatures can not be extracted from the present data here due to saturation effects. A low resolution 1D $T/T_{linear\ LIF}$ profile obtained at two positions in the wake of the model is presented and showed the expected behaviour. For the future it is important to examine new spectral line candidates in HEG that have been shown to be reliable in recent hot cell measurements. Quenching measurements have to be carried out for quantitative NO concentration determination and saturation of LIF has to be examined in hot cell measurements. Future 2D measurements retain the same geometry, but employ laser sheets. From this change we expect avoidance of saturation and better signal to noise ratio.

## 6. ACKNOWLEDGEMENTS

The authors thank all colleagues who have been associated with obtaining LIF results in the HEG. The financial support of the European Space Agency through CNES is also gratefully acknowledged.

## 7. REFERENCES

[1] D. Kastell, T.J. Horvath, G. Eitelberg, „Nonequilibrium Flow Expansion Experiment Around a Blunted Cone", 1994

[2] M. Scheer, „Temperature and density measurements on hypersonic wind tunnels using laser induced fluorescence of NO, including a study of NO

spectroscopy in the range 193-4 nm using a novel heated cell", Diploma thesis, May 1994.

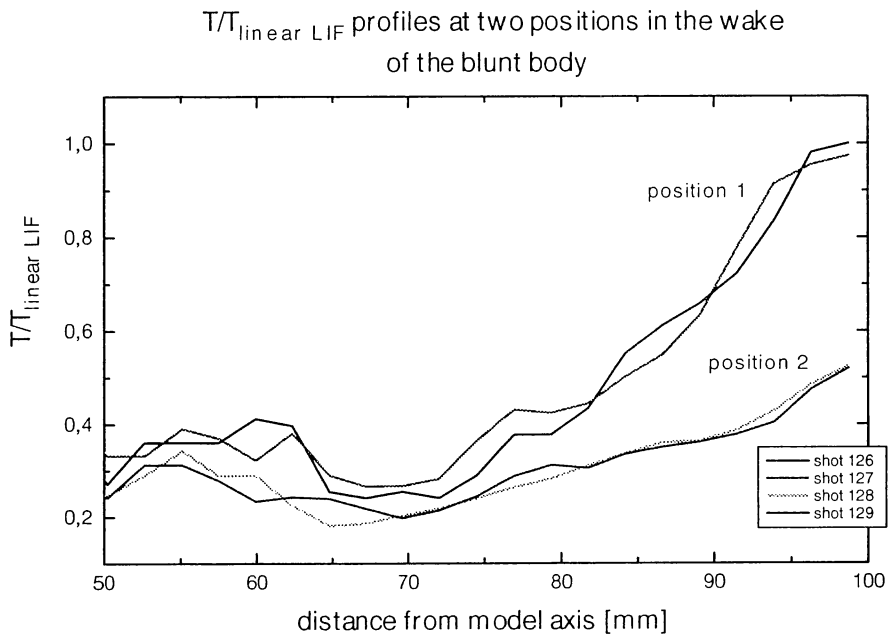


$T_{linear\ LIF}$ = 1800K (for linear LIF)

*Figure 5.*

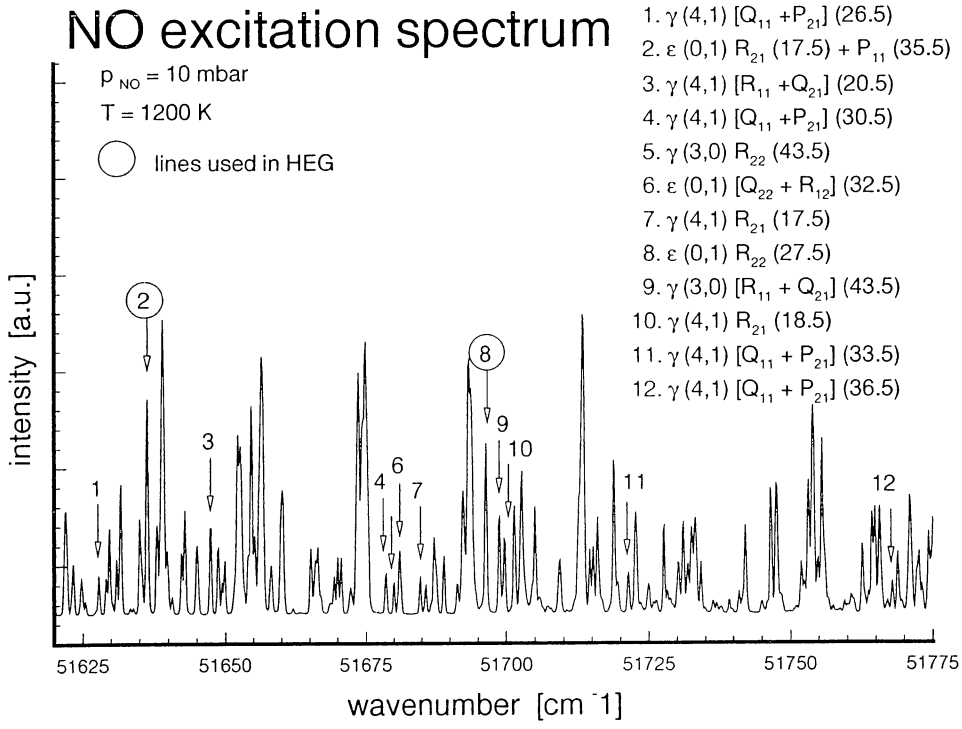


*Figure 6. Excitation spectrum of NO*

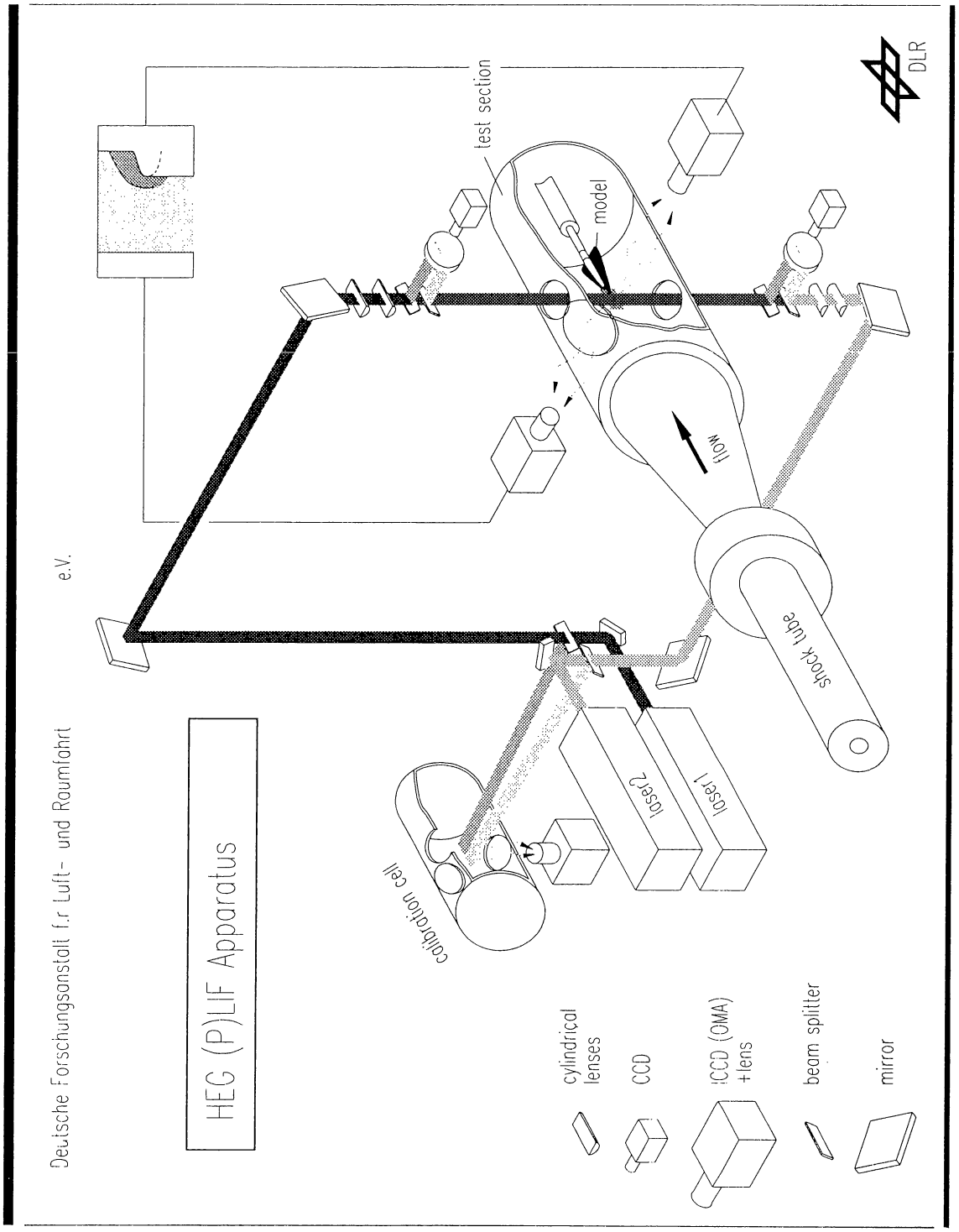


*Figure 7.*